Accuracy of Parameter Extraction from Sample-Averaged Sea-Echo Doppler Spectra

DONALD E. BARRICK, MEMBER, IEEE

Abstract—**The mean, standard deviation, and confidence limits are obtained for quotients of random-variable sums. Such quotients are formed in the extraction of sea-state parameters from high-frequency (HF) radar Doppler spectra. An equivalent chi-squared process is shown to represent a spectral integration having a varying mean based on central-limit theorem arguments. The error of estimating the centroid of a spectral peak is derived and shown to depend only on the total length of the time series, not on how it is segmented into coherent spectra and incoherent averages. Finally, error in estimation of waveheight using a power-law relationship is analyzed and is seen to depend on how one does the averaging. When individual spectra contain varying path losses and/or system gains, averages of quotients for each spectrum remove such unknown factors; in this case spectra with greater frequency resolution lead to lower waveheight estimation errors.**

INTRODUCTION

THE EXTRACTION of sea-state parameters from high-frequency (HF) radar sea-echo Doppler spectra involves comparison of one part of the spectrum with another (usually a division process, e.g., [1]-[5]). This eliminates the need to know the absolute signal level, a quantity difficult to ascertain because of varying path losses and system gains. Since the sea-surface height is (to first order) a Gaussian random variable, the received voltage echo is also Gaussian [6]. This means that the power output at each spectral point by the fast Fourier transform (FFT) is a chi-squared (χ^2) random variable with two degrees of freedom. (Each spectral point is statistically independent from every other in the absence of extensive overlap due to time series windowing [7]. Windowing with overlap can result in some correlation between adjacent points [8].) Division of sums of χ^2 power spectral samples produces another random variable which follows an F distribution [9]. Most of the results in this paper are derived from F-distribution properties.

Unfortunately, the utilization of F distributions by the radar remote-sensing community is virtually nonexistent, primarily because these distributions are discussed in textbooks as applied to statistical testing of hypotheses, e.g., whether the accuracies of the output of two different machines are similar [9]. As a result the notations developed in such treatments are ill-suited to the spectral estimation problems dealt with by radar analysts. Furthermore, many simple useful closed-form expressions can be derived (based on central-limit theorem arguments and binomial expansions) that are not usually found in treatments of F distributions.

In this paper we first present the χ^2 and F distributions in a natural notation for spectral analysis and give several of their properties such as moments and confidence limits. Then we discuss the problem of sums of χ^2 variables with unequal means and show that such sums can be represented by a χ^2 distribution whose equivalent number of independent samples is simply determined by these unequal means. This allows the immediate use of the desirable properties of χ^2 and F distributions. Then we apply these techniques to the problem of estimating the positional error of a spectral peak resulting from a finite number of samples. Finally, we examine various methods of sample averaging applied to the problem of extracting sea waveheight based on a power-law relationship for the F-distributed quotient of second-order to first-order spectral energy.

Manuscript received February 1, 1979; revised July 3, 1979.

The author is with the Sea State Studies Program Area in the Wave Propagation Laboratory, National Oceanic and Atmospheric Administration, U.S. Department of Commerce, Boulder, CO 80302.

χ^2 AND F DISTRIBUTIONS APPLIED TO SPECTRAL SAMPLES

Consider the sample average of L independent power spectral points U_l having the same mean, i.e., $\langle U_l \rangle = P$. Each spectral sample is χ^2 with two degrees of freedom, because the real and imaginary parts of the voltage signal output from the FFT, i.e., R_l and I_l, are Gaussian zero-mean independent random variables with $U_l = R_l^2 + I_l^2$ where $\langle R_l^2 \rangle = \langle I_l^2 \rangle = \frac{1}{2} P$. Let us normalize U_l dividing by P, i.e., $u_l = U_l/P$. Then the probability density function (pdf) for the sample average u can be expressed as

$$p_u(u) = \frac{L^L u^{L-1}}{\Gamma(L)} e^{-Lu}, \qquad \text{for } u > 0, \tag{1}$$

where

$$u = \frac{1}{L} \sum_{l=1}^{L} u_l. \tag{2}$$

The pth moment (p need not be an integer) of u is given as

$$\langle u^p \rangle = \int_{-\infty}^{\infty} u^p p_u(u)\, du = \frac{\Gamma(L+p)}{\Gamma(L) L^p}. \tag{3}$$

From this we immediately have the mean and standard deviation of u as

$$M(u) = \langle u \rangle = 1, \tag{4}$$

$$SD(u) = [\langle u^2 \rangle - \langle u \rangle^2]^{\frac{1}{2}} = 1/\sqrt{L}. \tag{5}$$

Now we similarly examine the statistics of q where q is the quotient of normalized χ^2 sample-averaged variables, the numerator x consisting of M samples, and the denominator y, of

N samples, i.e.,

$$q \equiv x/y = \frac{\frac{1}{M}\sum_{m=1}^{M} x_m}{\frac{1}{N}\sum_{n=1}^{N} y_n}, \tag{6}$$

where x and y each have pdf's of the form of (1). The non-normalized numerator and denominator samples would be defined by $X_m = x_m P_n$ and $Y_n = y_n P_d$, where the numerator and denominator variables all have means P_n and P_d, respectively. Furthermore, we assume that the numerator and denominator are statistically independent, i.e., that x_m is not equal to y_n for any m, n (or even correlated). Then the following transformation [10] is used to find the pdf for q:

$$p_q(q) = \frac{1}{q^2}\int_0^\infty p_x(w)p_y(w/q)w\,dw. \tag{7}$$

This yields

$$p_q(q) = \frac{M^M N^N \Gamma(M+N)}{\Gamma(M)\Gamma(N)} \cdot \frac{q^{M-1}}{(Mq+N)^{M+N}}, \qquad \text{for } q > 0. \tag{8}$$

The pth moment is given by

$$\langle q^p \rangle = \int_{-\infty}^{\infty} q^p p_q(q)\,dq = \left(\frac{N}{M}\right)^p \frac{\Gamma(M+p)}{\Gamma(M)} \frac{\Gamma(N-p)}{\Gamma(N)}, \tag{9}$$

from which we obtain the mean and standard deviation of q

$$M(q) = \frac{N}{N-1}, \tag{10}$$

$$SD(q) = \sqrt{\frac{N^2(M+N-1)}{M(N-1)^2(N-2)}}. \tag{11}$$

The above two expressions become infinite (and hence are meaningless measures of fluctuation) for $N = 1$ and $N = 1$, 2, respectively.

When N is large a particularly meaningful expression for the standard deviation is obtained:

$$SD(q) \underset{N \text{ large}}{\longrightarrow} \sqrt{1/M + 1/N}. \tag{12}$$

In the Appendix we show that in this limit of large N the F distribution becomes χ^2 with an effective number of independent samples, L_e, given by

$$1/L_e = 1/M + 1/N. \tag{13}$$

This fact is quite useful because the central-limit theorem of statistics [10] proves that the sum of random variables always approaches a Gaussian variable (regardless of the statistical distributions of the individual terms) so long as the number of terms is large. The above result shows that the quotient of large numbers of random variables therefore also approaches Gaussian so long as the number of *denominator* terms is large. Whenever Gaussian statistics can be used, closed-form expressions are usually obtainable because of the simplicity of manipulating Gaussian functions.

Note from (10) that the mean of q depends on N, the number of denominator samples, even though the separate means of numerator and denominator are unity. The quotient mean approaches unity only for large N.

Another measure of the fluctuation of a random variable is discussed in terms of "confidence limits." For example, symmetrical confidence limits $W^{(1)}$ and $W^{(2)}$, representing a probability $P = 0.9$ (i.e., 90 percent confidence), are taken to mean that there is a five-percent probability that the random variable w is either smaller than $W^{(1)}$ or larger than $W^{(2)}$; conversely, this means that we can be 90 percent certain that w lies between $W^{(1)}$ and $W^{(2)}$. Thus we formally define symmetrical confidence limits $W^{(1)}$ and $W^{(2)}$ for a given probability or confidence level P as

$$\int_{-\infty}^{W^{(1)}} p_w(w)\,dw = \tfrac{1}{2}(1-P)$$

$$= \int_{W^{(2)}}^{\infty} p_w(w)\,dw. \tag{14}$$

For a probability density function such as χ^2 or F there is usually no simple closed-form expression for confidence limits. Tables are available in the case of these two particular distributions, but considerable manipulation must be done in transforming to the sample-averaged spectral parameters we employ here. Hence, with computers it is just as convenient to calculate them using integration routines with (14). We plot such results for four cases: a) the χ^2 distribution given in (1) for the sample average of L power spectra, Fig. 1; b) the quotient of χ^2 distributions of M sample-averaged power spectra in the numerator to N sample-averaged power spectra in the denominator, defined in (8), where we take $M = N$, Fig. 2; c) same as b) except $M = 3N$, plotted versus N in Fig. 3; and d) same as b) except $N = 3M$, plotted versus M in Fig. 4. The confidence in all cases is 90 percent (symmetrical) and are shown as the upper and lower limits (i.e., $W^{(2)}$ and $W^{(1)}$) of the crosshatched region. These figures also give the mean of the random variable and lines showing the standard deviation on both sides of the mean.

Several points are worth noting from these figures. First, the regions of fluctuation (i.e., confidence limits and standard deviations) are always greater when *both* denominator and numerator fluctuate than when just the numerator fluctuates: compare Fig. 2 with Fig. 1. In particular, the upper limit for a small number of samples in the denominator becomes much larger, because the denominator is likely to approach zero causing the quotient to become large.

Second, note that the mean and standard deviations shown in Figs. 2 and 3 go to infinity when the number of denominator samples approaches 1 and 2, respectively. On the other hand, the confidence limits for this small number of samples always remain finite. It may seem surprising that the mean and standard and deviations, which always lie well inside the 90 percent confidence limits for larger sample averages, diverge for small samples while the confidence limits do not. This strange situation is due to the difference in the nature of the two methods of expressing fluctuation, i.e., moments versus confidence

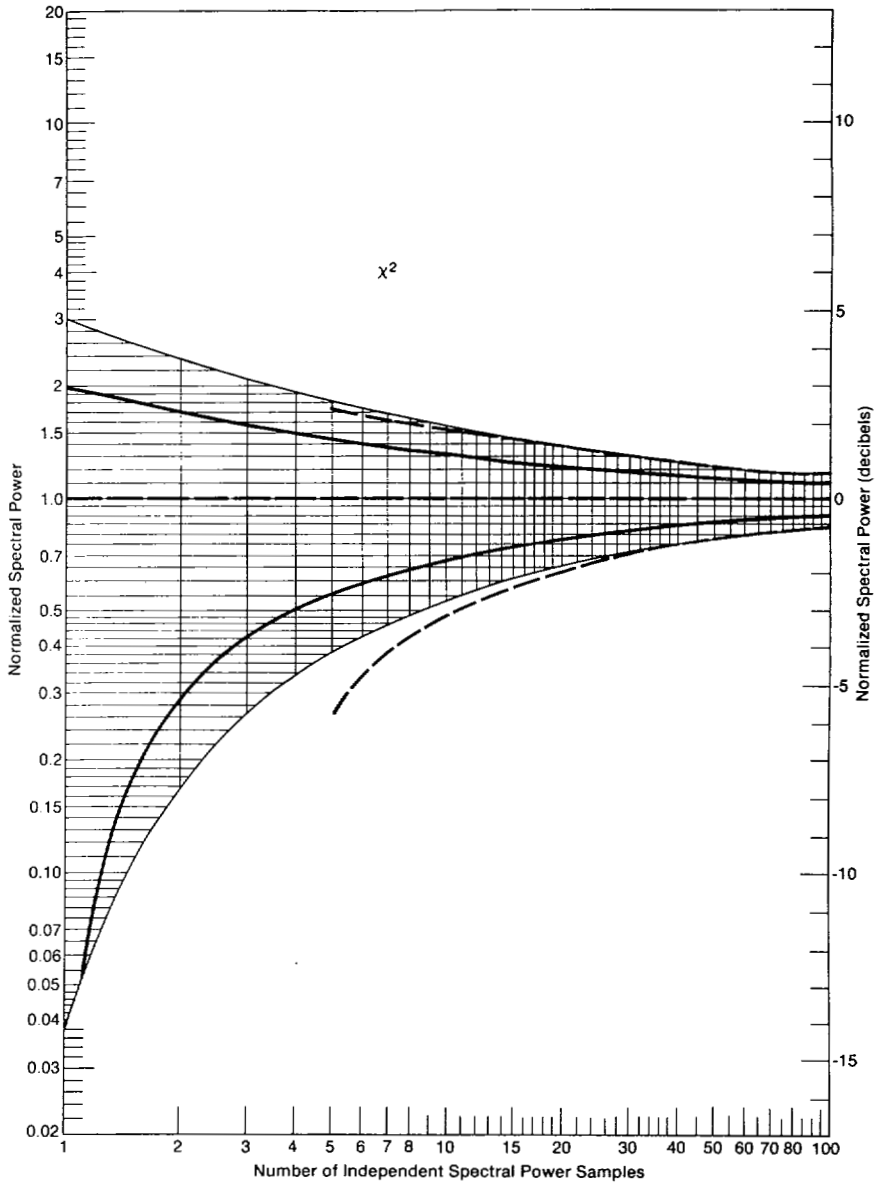

Fig. 1. Chi-squared fluctuation statistics versus number of independent spectral power samples. Outer boundaries of crosshatched area are 95 percent (upper) and 5 percent (lower) confidence limits; dashed lines are (16) as approximations to confidence limits. Heavy dashed line is mean, and heavy solid lines are ±1 standard deviation about mean.

limits. Hence, when there is only one sample in the numerator and denominator we cannot even define a mean value for the quotient; however, we can say that 90 percent of the time the quotient lies between 0.025 and 19.

Although a closed-form expression for the confidence limits does not exist for arbitrary M and N, we can derive a simple relationship when M and N become large. We have shown that when N is large q can be represented by a χ^2 distribution with an equivalent number of samples L_e, given by (13). This χ^2 variable is in turn the sum of L_e identical but independent variables. By the central-limit theorem the distribution of this sum tends toward Gaussian in the limit of large L_e. Thus the χ^2 distribution of (1) and also the F distribution of (8) *both* begin to take on the expected bell-shaped appearance of the Gaussian function for large M and N. Hence we can write an equivalent Gaussian probability density function for u in place of (1) and for q in place of (8) for large L (or M and N) whose mean tends to unity and whose variance tends to $1/L$ or $1/L_e$. Employing this density function we can define confidence limits in terms of the well-tabulated error function $\mathrm{erf}(z)$; we define an inverse error function, $\mathrm{erf}^{-1}(P)$, which is obtained from the tables by searching the erf (z) column for the value P and then finding the corresponding z. Then the confidence limits for large L_e are given by

$$W^{(2)} = 1 + \Delta, \qquad W^{(1)} = 1 - \Delta, \tag{15}$$

where

$$\Delta \equiv \frac{2}{L_e}\ \mathrm{erf}^{-1}(P), \tag{16}$$

where P is the symmetrical fractional confidence level desired. For the case considered here where $P = 0.9$ we find that $\mathrm{erf}^{-1}(0.9) = 1.163$, and hence $\Delta = 1.6447/\sqrt{L_e}$.

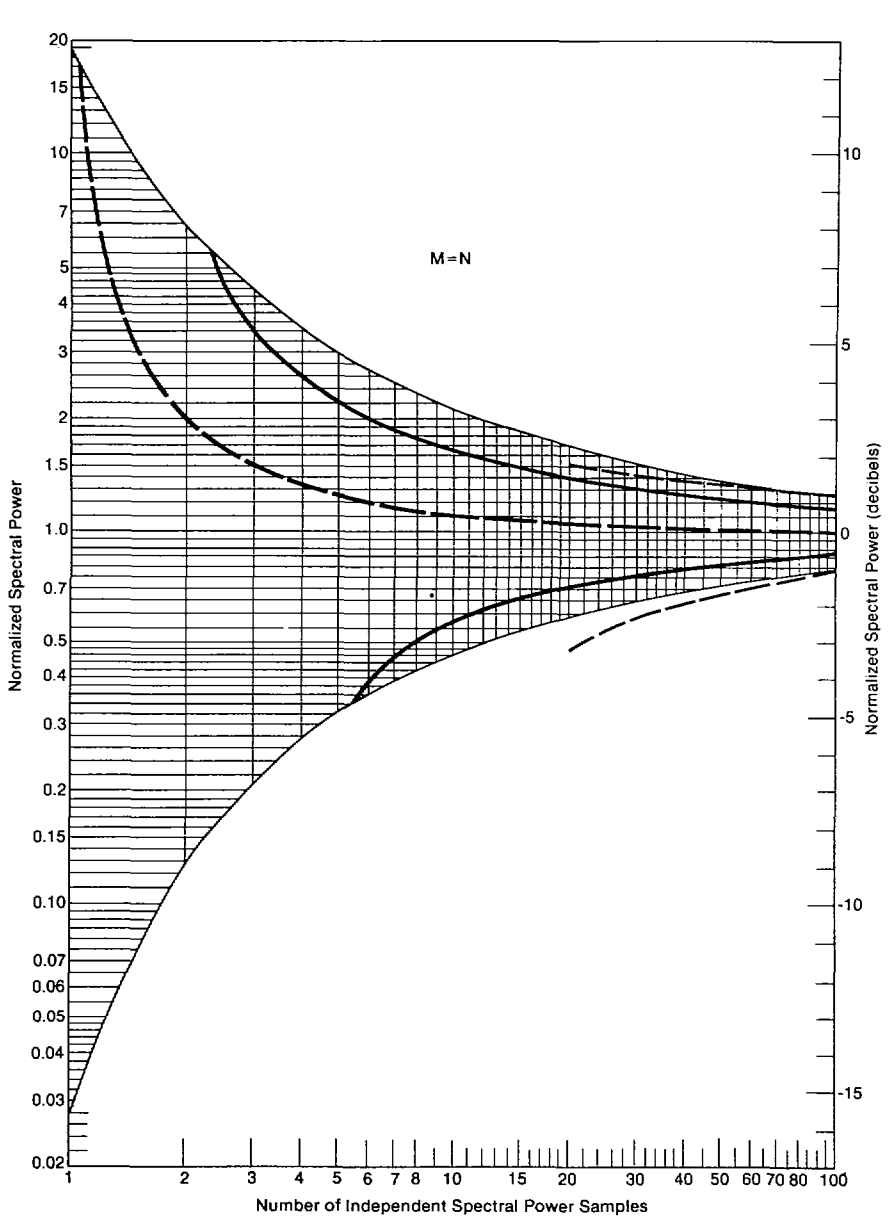

Fig. 2. F-distributed fluctuation statistics with same number of numerator and denominator samples versus number of independent spectral power samples in numerator or denominator. Curve legends same as Fig. 1.

To see how well this approximation holds up we have plotted it on Figs. 1-4 as the dashed line. For these four figures, respectively, we have a) $L_e = L$; b) $L_e = M/2 = N/2$; c) $L_e = 3N/4$; and d) $L_e = 3M/4$. It can be seen that this approximation to the confidence limits is quite valid even as low as $L_e = 20$.

EQUIVALENT NUMBER OF SPECTRAL SAMPLES

In all of the preceding discussions of χ^2 and F distributions it was assumed that the means of the individual spectral samples are the same. In many cases, however, it happens that the quantity to be used as numerator and/or denominator is actually the sum of random variables with unequal means. This is illustrated in Fig. 5, a sketch of a single HF Doppler spectrum. A frequently employed method of extracting waveheight takes the ratio of areas under different portions of the spectrum. This is realized by merely adding the spectral power samples at consecutive points. The dashed curve shows the (infinite-ensemble) mean of this spectral process, varying from point to point. One intuitively suspects that adding samples with different means is a smoothing process, and the resulting sum should be representable by an equivalent χ^2 sum with a determinable single variance and effective number of degrees of freedom.

An expression for the equivalent number of spectral samples is derived in the Appendix. Define L as the total number of spectral points having different variances to be summed in computing the area and K as the number of separate spectra to be sample averaged. Then the expression for the equivalent number of spectral samples L_e becomes increasingly accurate when KL_e is large (i.e., greater than ten), so that central-limit theorem arguments can be invoked. The result is

$$L_e = f \cdot [1 + p_2 + \cdots + p_L], \tag{17}$$

where $p_l \equiv P_l/P_M$, P_l being the power mean at the lth spectral

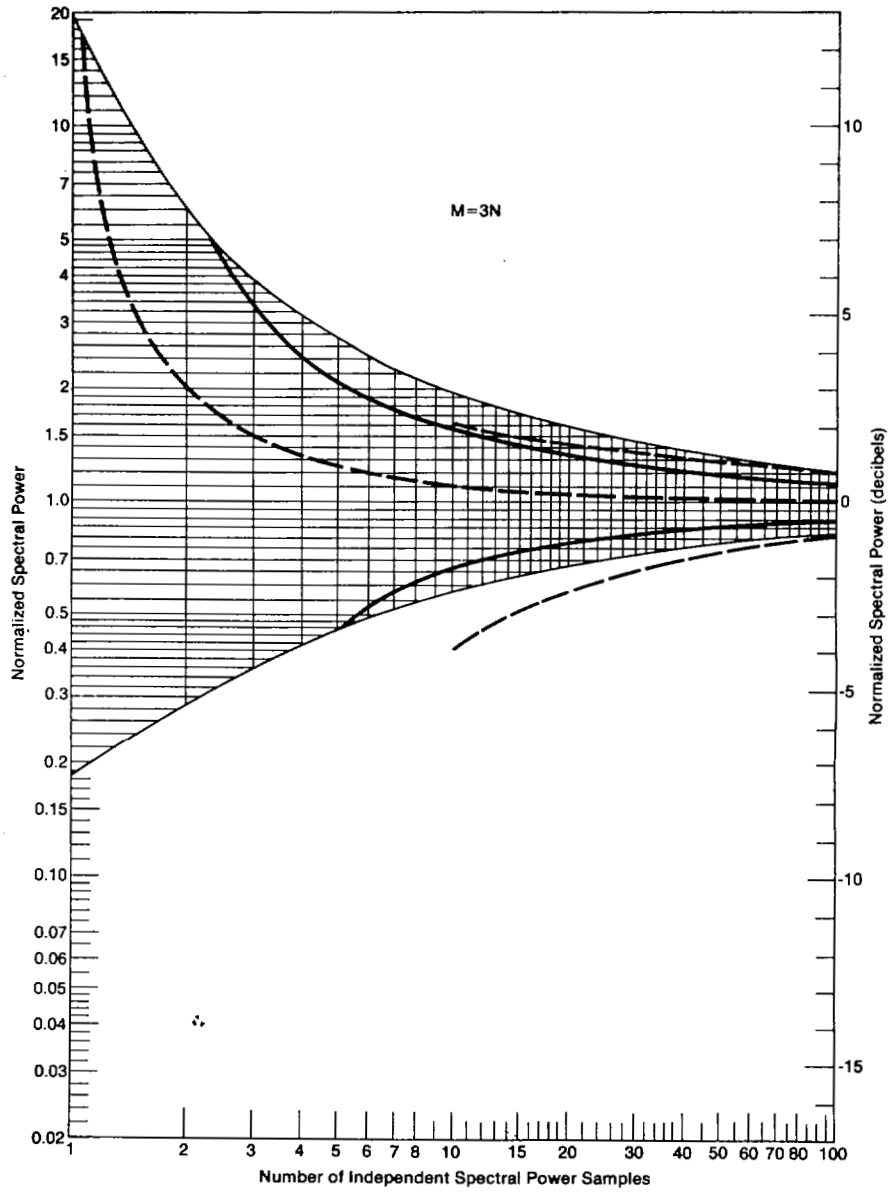

Fig. 3. *F*-distributed fluctuation statistics with three times as many numerator samples as denominator samples versus number of independent spectral power samples in denominator. Curve legends same as Fig. 1.

point and P_M being the maximum spectral power mean within the spectral region to be used. The expression in braces above has a simple physical interpretation: it is the number of spectral points included within the "half-power width" of the spectral regions of interest. ("Half-power width" is defined as $\Delta f = (\int P(f)\, df)/P_M$.) Thus if the means were all equal, i.e., $P_l = P_M$, we would merely have $L_e = L$ (with $f = 1$).

The quantity f is a shape factor that is close to unity. It is

$$f = \frac{1 + p_2 + \cdots + p_L}{1 + {p_2}^2 + \cdots + {p_L}^2}. \tag{18}$$

To obtain a range of typical values for the shape factor we approximate the summations in this ratio by integrals. Such a step is valid when the increment spacing is small in terms of the function half-power width. (In the other extreme where the increment spacing is much larger than the function width one readily sees that $f \cong 1$.) Then we derive f for the following five functions: 1) triangular function, $f = 1\frac{1}{2}$; 2) Gaussian function, $f = \sqrt{2}$; 3) cosine-squared function, $f = 1\frac{1}{3}$; 4) parabolic function, $f = 1\frac{1}{4}$; and 5) rectangular function, $f = 1$. We see that the more flattened the top of the function, the closer is f to unity. As a compromise estimate for the usual rounded-top spectral peak we suggest a value $f \cong 1.3$.

Thus a quick estimate of the equivalent number of spectral samples under a region of a single spectrum (adequate for accuracy estimation purposes) is obtained by counting the number of points within the half-power width[1] of this spectral region and multiplying by 1.3. For example, for the sketch of

[1] The "half-power width" as we have defined it in integral form is technically different from the width of the function between points at $P_M/2$, which we will call the 3-dB width. In practice this difference is small enough to be negligible. For example, for the five models given above (in that order), the ratios of the 3-dB width to the half-power width are 1) 1; 2) 0.94; 3) 1; 4) 1.06; and 5) 1.

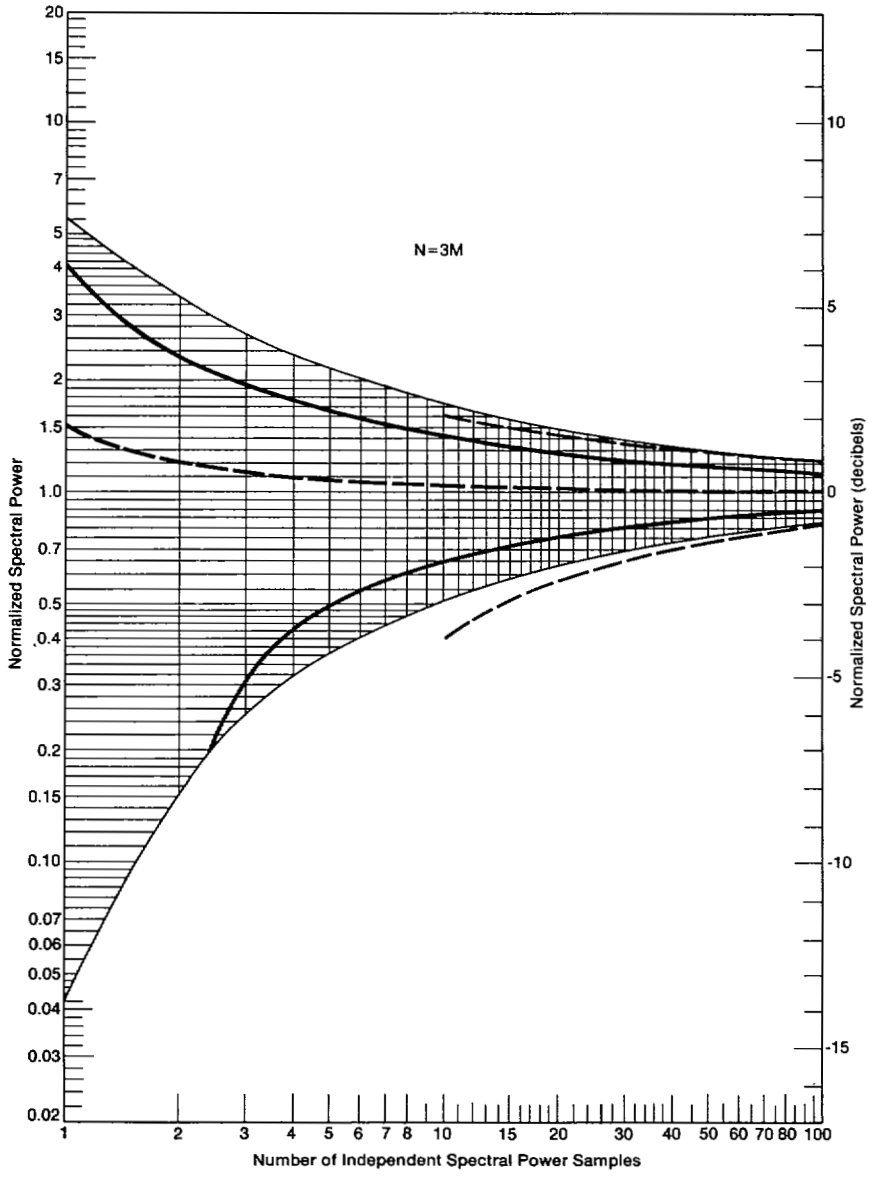

Fig. 4. *F*-distributed fluctuation statistics with three times as many demonimator samples as numerator samples versus number of independent spectral power samples in numerator. Curve legends same as Fig. 1.

Fig. 5, the equivalent number of first-order spectral samples is $N_e \cong 1.3 \times 5 \cong 7$. There are two sides comprising the second-order region whose maximum for the entire region P_{2M} occurs on the right side; the equivalent number of samples as shown in $M_e \cong 1.3 \times (10 + 7) \cong 22$.

CENTROID FREQUENCY ERROR FROM RANDOM SPECTRA

Many applications of HF radars to ocean remote sensing involve the estimation of the "mean" or center frequency of a spectral peak having narrow but finite width. Because each FFT power point within the spectral peak is χ^2 distributed with two degrees of freedom and there are K independent spectra to be averaged, any estimate of center frequency will contain error. There are many methods of defining the "mean" frequency of a peak; we select for analysis here the commonly used "centroid" definition. However, the "split-gate tracker" method of defining the mean frequency (in which the mean

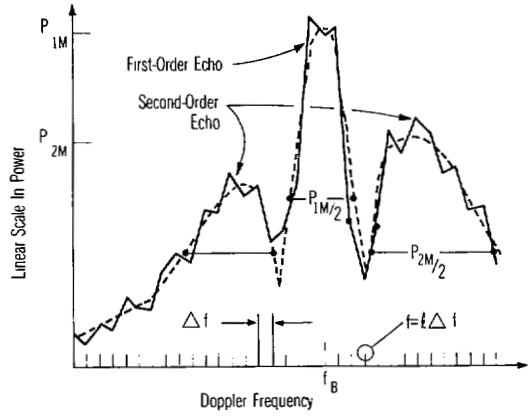

Fig. 5. Sketch of unaveraged FFT output (solid line) sea-echo Doppler spectral power versus discrete frequency points; each FFT point is chi-squared with two degrees of freedom whose (infinite-ensemble) mean is indicated by dashed line.

frequency divides two equal areas to its left and right within the spectral peak region) can be shown to yield the same final approximation as the centroid result derived here.

One example of the use of the peak frequency involves the estimation of the surface current with a narrow-beam radar from the position of the first-order spectral peak [11], [12]. In another example, the positions of four fairly narrow second-order peaks can be used to estimate the parameters of swell, such as its period, direction, and height [13].

The centroid definition of peak position is

$$\tilde{f} = \frac{\Delta f \sum l U_l}{\sum U_l} \tag{19}$$

where Δf is the spectral frequency resolution (or spacing between adjacent points), and hence $l\Delta f$ is the frequency position of the lth point, as shown in Fig. 5, within the desired spectral region (with respect to some convenient zero reference). Also, it is assumed that the spectral points U_l are already sample averaged from K separate spectra, i.e.,

$$U_l = \frac{1}{K} \sum_{k=1}^{K} U_{lk}. \tag{20}$$

In analyzing errors we assume for convenience symmetrical models for the means of U_l about the peak and define the true position of this peak as f_t. Hence we have $\langle U_l \rangle = \langle U_{-l} \rangle = P_l$, and take $l = 0$ as the position f_t of the true mean. Then in the Appendix we derive an expression for the standard deviation or rms error of $\tilde{f} - f_t$. This expression is valid for $KL_e \gg 1$, where L_e is the equivalent number of spectral samples in the desired spectral region as defined in the previous section. The result is

$$SD\left(\frac{\tilde{f}-f_t}{\Delta f}\right) = \frac{\sqrt{\frac{1}{K}\sum_l l^2 P_l^2}}{\sum_l P_l}, \tag{21}$$

where the summations are taken over the regions of interest (e.g., the first-order region of Fig. 5). As before, P_l represents the (infinite-sample) power average at the lth spectral point.

Although (21) is a general expression for the frequency estimation error, a simpler form can be obtained from this equation if one employs a model for the shape, a result that illustrates more clearly the parameter dependencies involved. We examine two models here to ascertain sensitivity to the form of the model.

1) *Rectangular Peak Shape:*

$$SD(\tilde{f} - f_t) = 0.58\, \Delta f \sqrt{N_h/K}. \tag{22}$$

2) *Gaussian Peak Shape:*

$$SD(\tilde{f} - f_t) = 0.50\, \Delta f \sqrt{N_h/K}. \tag{23}$$

In each of these expressions N_h is the number of samples contained within the half-power width of the respective pulse (as defined by the factor in square brackets of (17)), and K is the number of Doppler spectra used in the average. It is obvious that there is only a very weak dependence on pulse shape.

An interesting but not unexpected conclusion can be deduced from (22) and (23). For a given length time series it makes no difference how one divides the series up into consecutive FFT's to be incoherently averaged. For example, suppose we double the number of time series, each time series now being half as long. Then Δf increases by two, K increases by two, but N_h decreases by two. The net standard deviation in frequency position is therefore unchanged. If one wants to decrease the rms frequency error by a factor of two, he must increase the time-series length used by a factor of four.

ACCURACY OF VARIOUS AVERAGES FOR WAVEHEIGHT EXTRACTION

The most important single parameter characterizing "sea state" is the rms waveheight.[2] Therefore we illustrate the use of the above statistical relationships in assessing the accuracy of various possible averaging schemes one might consider for waveheight extraction. The techniques illustrated here can be applied analogously to other inversion methods for extracting additional sea-state parameters.

The general form of the equation for waveheight extraction is

$$k_0 h = CR^p, \tag{24}$$

where k_0 is the radar wavenumber, h is the rms ocean waveheight, C and p are constants, and R is a ratio of second-order Doppler spectral energy to the first-order energy. Barrick [1] originally derived a model in which the second-order spectral points of the numerator of R were divided by a known weighting function; in that case he showed that $p = \frac{1}{2}$. Maresca and Georges [5] have suggested an empirical model in which the numerator of R is the simple unweighted second-order spectral power. For their model they found that $p \cong 0.6$ provided a best fit over most of the region of interest. Hence the range of p for waveheight extraction considered here lies between zero and unity.

Normally with a surface-wave radar which collects K sequential spectra in time at a given range one would merely sample average all K spectra. Thus if the numerator (or second-order spectral area) consists of M equivalent samples (as defined previously) and the denominator (or first-order spectral area) consists of N equivalent samples, then the total numerator and denominator would consist of KM and KN samples, respectively. It is shown below that this method of averaging provides the best possible accuracy. However, there are cases (with skywave radar, for example) when consecutive Doppler spectra in range or time may be multiplied by an unknown but varying path loss or system gain. In such a case it would be desirable to eliminate the unknown constant *before* averaging. One method is to divide the second-order area by the first-order area for *each* spectrum before sample averaging similar quotients from all K spectra. There are several variations on this scheme analyzed below. In all the following K (the number of spectra) is assumed to be large, while M and N need not be. We derive in the Appendix and present below two quantities: $sd(h)$ is the *normalized* standard deviation of waveheight (or its rms percent $\times$ 100 error), and h_b/h is the waveheight bias due to sampling (i.e., h_b is the recovered rms waveheight while h is the true input rms waveheight). After presenting the

[2] The "significant waveheight," a term used traditionally by oceanographers, is four times the rms waveheight.

formulas for these errors in each case, we show an example for illustration.

A. Separate Total Averaging of Numerator and Denominator

In this most obvious method we form the waveheight estimate for (24) with the numerator and denominator samples X_i and Y_j as follows:

$$k_0 h = CR^p, \qquad \text{where } R = \frac{\frac{1}{KM}\sum_{k,m=1}^{KM} X_{km}}{\frac{1}{KN}\sum_{k,n=1}^{KN} Y_{kn}}. \tag{25}$$

For this case the error and bias are

$$sd(h) = p\sqrt{1/KM + 1/KN}\,, \qquad h/h_b = 1. \tag{26}$$

Since KM and KN are large it makes no difference whether the number of numerator samples is larger or smaller than the number of denominator samples here. In what follows it *does* matter.

B. Average of Quotient for Each Power Spectrum

Here we form the quotient of second-order to first-order area for each power spectrum, sample-average this K times, and raise the result to the pth power. Hence,

$$k_0 h = CQ^p,$$

where

$$Q = \frac{1}{K}\sum_{k=1}^{K} Q_k,$$

and

$$Q_k = \frac{\frac{1}{M}\sum_{m=1}^{M} X_{km}}{\frac{1}{N}\sum_{n=1}^{N} Y_{kn}}. \tag{27}$$

The error and bias for this case are

$$sd(h) = p\,\langle q\rangle^{p-1} SD(q)/\sqrt{K}, \qquad h_b/h = \langle q\rangle^p, \tag{28}$$

where the mean and standard deviation of q required in these equations are given in (10) and (11).

C. Average of Quotient to pth Power for Each Spectrum

In this variation of the preceding technique we first raise the quotient for each power spectrum to the pth power and then take the K sample average:

$$k_0 h = CQ^{(p)}, \qquad \text{where } Q^{(p)} = \frac{1}{K}\sum_{k=1}^{K} Q_k{}^p,$$

and where

$$Q_k = \frac{\frac{1}{M}\sum_{m=1}^{M} X_{km}}{\frac{1}{N}\sum_{n=1}^{N} Y_{kn}}. \tag{29}$$

The error and bias for this case are

$$sd(h) = SD(q^p)/\sqrt{K}, \qquad h_b/h = \langle q^p\rangle, \tag{30}$$

where the mean and standard deviation of q^p are obtained from the general moment expression (9). For $0 < p < 1$, the error and bias for this method are less than for the preceding method.

D. Average of Reciprocated Quotient for Each Power Spectrum

Our previous results as summarized in (11) show that better stability is obtained for a larger number of denominator samples. In the case of sea-echo spectra, such as that sketched in Fig. 5, the number of denominator samples N is always less than the number of numerator samples M. This suggests the following: reciprocate the quotient, sample-average this quantity, raise it to the pth power, and then reciprocate again. Thus,

$$k_0 h = CG^{-p},$$

where

$$G = \frac{1}{K}\sum_{k=1}^{K} G_k,$$

and

$$G_k = \frac{\frac{1}{N}\sum_{n=1}^{N} Y_{kn}}{\frac{1}{M}\sum_{m=1}^{M} X_{km}}. \tag{31}$$

The error and bias here are

$$sd(h) = \frac{pSD(g)}{\langle g\rangle^{p+1}\sqrt{K}}, \qquad h_b/h = \langle g\rangle^{-p}, \tag{32}$$

where the mean and standard deviation of g are also given by (10) and (11), but with M and N now interchanged. It can be seen that for $M > N$, this method yields less error than B.

E. Average of Reciprocated Quotient to pth for Each Spectrum

The final variation on the above schemes is to raise the reciprocated quotient to the pth before sample averaging, i.e.,

$$k_0 h = C[G^{(p)}]^{-1},$$

where

$$G^{(p)} = \frac{1}{K}\sum_{k=1}^{K} G_k{}^p,$$

TABLE I

Averaging Method	A	B	C	D	E
Waveheight standard deviation (normalized percent)	4.33%	∞	7.24%	4.84%	4.60%
Waveheight bias factor	1.005	1.414	1.215	0.866	0.960

and

$$G_k = \frac{\frac{1}{N}\sum_{n=1}^{N} Y_{kn}}{\frac{1}{M}\sum_{m=1}^{M} X_{km}}. \tag{33}$$

Here we obtain

$$sd(h) = SD(g^p)/(\langle g^p\rangle^2\sqrt{K}), \qquad h_b/h = \langle g^p\rangle^{-1}, \tag{34}$$

where again the mean and standard deviation of g^p are obtained from (9) by interchanging the roles of M and N. For $M > N$ and $0 < p < 1$, this technique yields less error than the preceding three methods.

F. Example

To illustrate the magnitudes of the errors expressed functionally above we choose an example with the following parameters: $M = 4$, $N = 2$, $K = 100$, and $p = \frac{1}{2}$. Table I summarizes the normalized error and bias for this case. Thus we see that method E comes closest to the ideal, i.e., A, for all those cases where the quotient must be taken before sample averaging. Reciprocating before averaging is always best when $M > N$. (Note that if we had wrongly neglected the denominator fluctuation, ending up with a χ^2 distribution of KM samples, the predicted normalized error would have been $p/\sqrt{KM}$, or 2.5 percent here, considerably underestimating the true error.)

A final trade-off is worth noting. In method A it makes no difference in accuracy into how many consecutive spectra a time series of given length is divided. For example, if the time series is divided into twice as many spectra (so that K increases by two), then the frequency resolution decreases by two (so that both M and N decrease by two); hence the standard deviation given in (26) remains the same. On the other hand, if one uses any of the remaining four averaging methods, accuracy always increases by having more M and N samples. This is accomplished by increasing the frequency resolution (decreasing Δf) at the expense of fewer spectral averages K. By increasing M and N sufficiently (thereby decreasing K) one can approach the ideal given by (26).

CONCLUSION

This paper derives and demonstrates the use of χ^2 and F distributions for HF sea-echo Doppler spectra, where quotients of χ^2 variates must often be taken in extracting sea-state parameters. It is shown how the mathematics can very often be reduced to simple closed-form expressions exhibiting the dependence of sampling errors upon the relevant physical parameters. This reduction is effected, even in the case of the F-distribution quotient, by utilizing binomial expansions of the denominator and then invoking central-limit theorem arguments to show that all these results tend toward Gaussian.

The χ^2 quotients considered herein employ scalar division. At present investigations are underway in which the wave-height directional spectrum is obtained by integral inversion of the second-order Doppler spectrum after normalization by the first-order echo spectrum [3], [4], [7]. This normalization is essentially a division process also but in some cases involves tensors or matrices rather than scalar functions. Although the reworking of the above statistics with tensor rather than scalar algebra for this situation seems formidable, general estimates of the order of magnitudes of errors and their dependences on the relevant parameters can be based on the above scalar analyses. More accurate error analyses would probably require Monte Carlo techniques.

Finally, although our analysis has emphasized application to HF sea-echo Doppler spectra, the techniques and results are general and can be applied equally well to any geophysical problem where the radar echo is a random variable. Another application is wind measurement from microwave radars where echoes are obtained from clear-air turbulence [14].

APPENDIX

Expansion of (11) for large N leads directly to (12); there is another physically meaningful way of obtaining (12) for large N, however. We can represent the normalized quotient (6) as follows:

$$q = \frac{x}{y} = \frac{1 + \Delta_M}{1 + \Delta_N}, \tag{A1}$$

where $\langle\Delta_M\rangle = \langle\Delta_N\rangle = 0$, and it is easy to show that $SD(x) = SD(\Delta_M) = 1/\sqrt{M}$ and $SD(y) = SD(\Delta_N) = 1/\sqrt{N}$. Hence it is obvious that the fluctuation of Δ_N becomes small compared to unity as N becomes large. Thus expanding the denominator in a binomial series we obtain

$$q \cong 1 + \Delta_M - \Delta_N, \tag{A2}$$

where the remainder omitted above is of order $\Delta_N{}^2$. We see therefore that the fluctuating part of q is *larger* than either the numerator or denominator fluctuations alone, especially since the numerator and denominator are independent. Furthermore, we can assign $\Delta_e \equiv \Delta_M - \Delta_N$, and we see by comparison with x or y in (A1) that (A2) to lowest order has the form of χ^2 with total fluctuation Δ_e. Since $\langle\Delta_e{}^2\rangle = \langle\Delta_M{}^2\rangle + \langle\Delta_N{}^2\rangle = 1/M + 1/N$, we have established (12) independently as an equivalent χ^2 process for an F distribution with large N.

We establish the equivalent number of independent samples, as given by (17), by invoking central-limit theorem arguments. If we have K independent power spectra, then the K sample-averaged area under the spectral region of interest is given by $\Sigma U_l \equiv A$, where U_l is given by $U_l = (1/K)\Sigma_{k=1}^{K} U_{lk}$, with $\langle U_{lk}\rangle = \langle U_l\rangle = P_l$, and P_M as discussed after (17) is the maximum of all the means P_l. Assuming that the U_{lk} are statistically independent, we argue that for KL_e large (i.e., L_e being the equivalent number of spectral points in the A summation, to be defined subsequently), the central-limit theorem shows that the distribution of A tends toward Gaussian. We define L_e from the mean and variance of this Gaussian distribution (viz., L_eP_M and $L_eP_M{}^2/K$, respectively), because they are the means and variances of a χ^2 pdf for A

having equal means of P_M at all spectral points. The χ^2 tends toward Gaussian in the limit of many samples. We set these newly defined means and variances equal to the actual mean and variance of A, i.e., $P_M[1 + p_2 + \cdots +]$ and $P_M{}^2[1 + p_2{}^2 + \cdots]/K$, respectively. Then solving for the total equivalent degrees of freedom in the new distribution, we obtain

$$L_eK = f \cdot K[1 + p_2 + \cdots], \tag{A3}$$

with f as defined in (18).

In order to obtain (21) we re-express (19) in an incremental manner similar to (A1), where $l = 0$ corresponds to the position at the true peak center f_t. Thus we have

$$\frac{\tilde{f}-f_t}{\Delta f} = \frac{1 \cdot P_1(1+\Delta_{1K}) + \cdots + lP_l(1+\Delta_{lK}) + \cdots}{\cdots + P_{-l}(1+\Delta_{-lK}) + \cdots + P_l(1+\Delta_{lK}) + \cdots} - \frac{1 \cdot P_{-1}(1+\Delta_{-1K}) + \cdots + lP_{-l}(1+\Delta_{-lK}) + \cdots}{\cdots + P_{-l}(1+\Delta_{-lK}) + \cdots + P_l(1+\Delta_{lK}) + \cdots}, \tag{A4}$$

where it is assumed that the power spectrum at each frequency point l has been sample averaged K times. Assume that the range of l over which P_l lies within 3 dB of P_M is given by L_e and that $L_eK \gg 1$. Then the denominator can be expanded in binomial fashion, yielding

$$\frac{\tilde{f}-f_t}{\Delta f} = \frac{\sum_{l=1}^{L_r} lP_l(\Delta_{lK} - \Delta_{-lK})}{\sum_{l=-L_r}^{L_r} P_l}, \tag{A5}$$

where $P_l = P_{-l}$ because of our symmetry assumption, and L_r is the outer bound of the spectral region to be included in the centroid analysis. Notice that (A4) is not strictly an F distribution; F distributions have uncorrelated numerators and denominators, which is violated by (A4). Use of the binomial expansion permits reduction to the χ^2 form (A5), obviating the difficulty of numerator and denominator correlation. Taking the standard deviation of (A5), one then arrives at (21). One could have retained terms of order Δ^2 in (A5) using the binomial expansion, but it can be shown that they will cancel in the standard deviation expression to lowest order.

We can derive (26) from (25) by use of (9) for $\langle q^p \rangle$. For large M and N, the gamma-function ratios there can be expanded asymptotically using Stirling's formula [15] and also the following expression:

$$\left(1 + \frac{p}{M}\right)^M \underset{M\to\infty}{\to} e^p(1 - p^2/2M), \tag{A6}$$

to obtain

$$\frac{\Gamma(M+p)}{\Gamma(M)} \underset{M\to\infty}{\to} M^p(1 + p/M)^{p-1/2}(1 - p^2/2M), \tag{A7}$$

$$\frac{\Gamma(N-p)}{\Gamma(N)} \underset{N\to\infty}{\to} N^{-p}(1 - p/N)^{-p-1/2}(1 - p^2/2N). \tag{A8}$$

Employing these, we arrive at (26).

Equation (28) is derived from (27) by using the representation $Q = (P_n/P_d)\langle q \rangle [1 + \Delta_K]$, where K is assumed large. P_n and P_d are the numerator and denominator power mean maxima; they cancel in the normalizing processes leading to fractional errors. Raising this to the pth power, using the binomial expansion, and taking the standard deviation yields (28).

Derivation of (30) from (29) is very straightforward. Equation (32) is obtained from (31) by binomial expansion methods as in the preceding paragraph, where we represent G as $G = (P_d/P_n)\langle g \rangle [1 + \delta_K]$, and then take the variance of G^{-p}, expressing this in terms of averages of $\delta_K{}^2$. Use is made of the fact that $\mathrm{SD}(g) = \sqrt{\langle \delta_K{}^2 \rangle}$. Finally, (34) proceeds from (33) along identical lines.

ACKNOWLEDGMENT

Many helpful and encouraging suggestions from Dr. Belinda Lipa of SRI International are greatly appreciated; enlightening discussions with Jack Riley of our laboratory are gratefully acknowledged.

REFERENCES

[1] D. E. Barrick, "Extraction of wave parameters from measured HF sea-echo Doppler spectra," *Radio Sci.*, vol. 12, pp. 415–424, 1977a.

[2] ——, "The ocean waveheight nondirectional spectrum from inversion of the HF sea-echo Doppler spectrum," *Remote Sensing of Environment*, vol. 6, pp. 201–227, 1977b.

[3] B. J. Lipa, "Derivation of directional ocean-wave spectra by integral inversion of second-order radar echoes," *Radio Sci.*, vol. 12, pp. 425–434, 1977.

[4] ——, "Inversion of second-order radar echoes from the sea," *J. Geophys. Res.*, vol. 83, pp. 959–962, 1978.

[5] J. W. Maresca and T. M. Georges, "HF skywave measurement of the ocean wave spectral parameters," *J. Geophys. Res.*, accepted for publication, 1980.

[6] D. E. Barrick and J. B. Snider, "The statistics of HF sea-echo Doppler spectra," *IEEE Trans. Antennas Propagat.*, vol. AP-25, no. 1, pp. 19–28, Jan. 1977.

[7] D. E. Barrick and B. J. Lipa, "A compact transportable HF radar system for directional coastal wave field measurements," in *Ocean Wave Climate*, M. D. Earle and A. Malahoff, Eds. New York: Plenum, 1978, pp. 153–201.

[8] F. J. Harris, "On the use of windows for harmonic analysis with the discrete Fourier transform," *Proc. IEEE*, vol. 66, pp. 51–83, 1978.

[9] S. Brandt, *Statistical and Computational Methods in Data Analysis*. Amsterdam: North Holland, 1970.

[10] A. Papoulis, *Probability, Random Variables, and Stochastic Processes*. New York: McGraw-Hill, 1965.

[11] D. E. Barrick *et al.*, "Sea backscatter at HF: Interpretation and utilization of the echo," *Proc. IEEE*, vol. 62, pp. 673–680, 1974.

[12] R. H. Stewart and J. W. Joy, "HF radio measurements of surface currents," *Deep Sea Res.*, vol. 21, pp. 1039–1049, 1974.

[13] B. J. Lipa and D. E. Barrick, "Methods for extraction of long-period ocean-wave parameters from narrow-beam HF radar sea echo," *Radio Sci.*, accepted for publication, 1980.

[14] E. E. Gossard *et al.*, "Observation of winds in the clear air using FM-CW Doppler radar," *Radio Sci.*, vol. 13, pp. 285–289, 1978.

[15] M. Abramowitz and I. A. Stegun, *Handbook of Mathematical Functions*. Washington, DC: GPO, 1964, ch. 6.

Donald E. Barrick (M'72) received the B.S.E.E. degree, the M.Sc. degree, and the Ph.D. degree in electrical engineering, all from Ohio State University, Columbus.

He was formerly a Fellow with Battelle's Columbus Laboratories and an Adjunct Assistant Professor of Electrical Engineering at the Ohio State University. At Battelle he directed programs in radar research and analysis, and he is coauthor of the *Radar Cross Section Handbook*, as well as the author of some 50 open literary publications. He is currently Chief of the Sea-State Studies Program Area in the Wave Propagation

Laboratory, National Oceanic and Atmospheric Administration, Boulder, CO. In 1971 he received the Sigma Xi Regional Outstanding Young Scientist Award, and in 1972 he was given the IEEE TRANSACTIONS ON ANTENNAS AND PROPAGATION Best Paper Award. He received the NOAA Outstanding Paper Award for 1978. Also, in 1978 he was awarded the U.S. Department of Commerce Gold Medal for development of a real-time HF radar system that maps ocean surface currents in coastal waters.

Dr. Barrick has served as Secretary of URSI's Commission F, has been a member of the Administrative Committee for the IEEE Antennas and Propagation Society, and has served as the Associate Editor for Geophysical Scattering and Propagation for the IEEE TRANSACTIONS ON ANTENNAS AND PROPAGATION.

Full-Wave Solutions for the Scattered Radiation Fields from Rough Surfaces with Arbitrary Slope and Frequency

EZEKIEL BAHAR, SENIOR MEMBER, IEEE

Abstract—**Full-wave solutions are derived for the scattered radiation fields from rough surfaces with arbitrary slope and electromagnetic parameters. These solutions bridge the wide gap that exists between the perturbational solutions for rough surfaces with small slopes and the quasi-optics solutions. Thus it is shown, for example, that for good conducting boundaries the backscattered fields, which are dependent on the polarization of the incident and scattered fields at low frequencies, become independent of polarization at optical frequencies. These solutions are consistent with reciprocity, energy conservation, and duality relations in electromagnetic theory. Since the full-wave solutions account for upward and downward scattering, shadowing and multiple scatter are considered. Applications to periodic structures and random rough surfaces are also presented.**

I. INTRODUCTION

THE PROBLEM of electromagnetic wave scattering by rough surfaces has been studied extensively because of its broad applications in science and technology. However, because of the complexity of the problem, satisfactory solutions are available only when very stringent restrictions are made on the rough surface profile, the electromagnetic parameters of the irregular boundary, or the frequency of the electromagnetic wave. Thus different solutions are derived depending on the approximate assumptions made to facilitate the analysis, and there are many pertinent scattering problems for which valid solutions are not available. For example, using a perturbational approach derived for surfaces with small gradients, the backscattered fields are shown to be strongly dependent upon the polarization of the incident and scattered waves [16]-[18]. Physical-optics solutions that are restricted to high frequencies indicate that for perfectly conducting surfaces the backscattered fields are not dependent on polarization [14].

A full-wave approach has been developed to remove the restrictions imposed on the earlier solutions. Thus complete expansions of the fields in terms of a basis consisting of the radiation, lateral, and surface-wave terms were used, and exact boundary conditions were imposed at the irregular boundary [4]-[7]. Using the orthogonal properties of the basis functions and employing Green's theorems to avoid differentiation of the field expansions at the irregular boundary, Maxwell's equations were converted into rigorous sets of ordinary coupled first-order differential equations for the forward and backward wave amplitudes. In order to cast the full-wave solutions in a form that could be readily used by the engineer and compared with earlier results, the coupled differential equations were converted into integral equations that were solved using a second-order iterative approach. Using these solutions some of the discrepancies existing in the earlier solutions were examined, such as reciprocity, energy conservation, scattering when the incident wave is near the Brewster angle, and when the incident or scattered waves are near grazing angles. Furthermore, coupling between the radiation fields and the surface and lateral waves (disregarded in earlier solutions) was also examined in detail [8], [9].

However, due to the iterative approach used to obtain the simple solutions they were restricted to moderately small slopes, and the transition between the perturbational approach and the quasi-optics approach was not clearly shown. In order to remove the restriction and to retain the relatively simple form of the final solution, in this work the rough surface is regarded as a continuum of elementary strips of varying slope and height rather than a continuum of elementary horizontal strips of varying height. It has been shown that the full-wave approach is most amenable to an iterative solution when it is based on a local modal analysis that conforms most closely to the varying parameters of the irregular waveguide [2], [3], [11], [12]. Thus, starting with the full-wave expression for the scattered fields by an elementary horizontal strip and performing the necessary coordinate transformations, the desired expressions are derived for scattering by a continuum of elementary strips of varying slope and height.

The small-slope approximations of these full-wave solutions agree with the earlier perturbational solutions, while the high-frequency approximations of the full-wave solutions agree with the physical-optics solutions for perfectly conducting boundaries. The solutions are shown to satisfy reciprocity, energy conservation, and duality relations in electromagnetic theory. The full-wave solutions account for both upward and downward scattering; thus, multiple scattering and shadowing effects can be considered. The radiation term is shown to

Manuscript received November 21, 1978; revised June 29, 1979. This work was supported by the U.S. Army Research Office and the Engineering Research Center at the University of Nebraska, Lincoln. This paper was presented at the AGARD conference on Terrain Profiles and Contours in EM Propagation, Norway, September 1979.

The author is with the Department of Electrical Engineering, University of Nebraska, Lincoln, NE 68588.

0018-926X/80/0100-0011$00.75